Molecular Vision 2014; 20:1569-1578 <http://www.molvis.org/molvis/v20/1569>
Received 18 March 2014 | Accepted 3 November 2014 | Published 5 November 2014

Age-dependent increase in miRNA-34a expression in the posterior pole of the mouse eye

Zeljka Smit-McBride, Krisztina I. Forward, Anthony T. Nguyen, Matthew H. Bordbari, Sharon L. Oltjen, Leonard M. Hjelmeland

UC Davis School of Medicine, Department of Ophthalmology, Vitreoretinal Research Lab, Davis, CA

Purpose: MicroRNA-34a (miR-34a) has been implicated in neurodegeneration. MiR-34a belongs to a signaling network involving p53 and Sirt-1. This network responds to DNA damage with further downstream signals that induce senescence or apoptosis. Our goal was to measure the expression level of miR-34a in the mouse retina and RPE as a function of age.
Methods: The age-dependent change in miR-34a expression was quantified using a real-time PCR (RT-PCR) assay on microRNA isolates from eye tissue: the retina and RPE/choroid (4, 18, 24, and 32 months of age). Tissue localization of miR-34a was determined by in situ hybridization (ISH) for a series of time points. Expression of the miR-34a target gene Sirt1 was analyzed using RT-PCR and immunohistochemistry.
Results: MiR-34a examined with real-time PCR showed a linear increase in expression with age when compared to that of 4-month-old mice. However, the level of expression between the 24 and 32-month-old animals showed mild down-regulation. An age-related increase in miR-34a expression was confirmed in the mouse eye using in situ hybridization. An inverse relationship between the levels of expression of miR-34a and its target Sirt1 mRNA was found at 18 and 24 months of age.
Conclusions: Our data showed that miR-34a expression increased in the retina and RPE with age. The level of DNA damage in mitochondria in the retina and RPE followed a similar time course. This suggests that miR-34a may play a role in the senescence and apoptosis of the retina and RPE cells in the aging eye.

MicroRNAs (miRNAs) are small non-coding RNAs that regulate gene expression at the post-transcriptional level and inhibit the translational initiation step by binding to the 3′ untranslated region (UTR) of their target message. MiRNAs have emerged as critical regulators of many biologic processes involved in developmental biology such as cell cycle control, apoptosis, and stem cell differentiation [1]. Their roles in the aging process have only recently been revealed following the discovery of miRNAs that regulate the lifespan in the nematode *Caenorhabditis elegans* [2]. Several miRNAs involved in the aging process have been identified: miR-127 regulates senescence of endothelial cells [3], miR-21 has been identified as a new circulating marker of inflammaging [4], and miR let-7 plays a role in tissue homeostasis, repair, and stem cell aging [5].

The literature suggests that circulating miRNAs have relevant diagnostic and prognostic implications for age-related diseases, but the clinical relevance is still controversial. Age-related upregulation of miR-34a in the blood and the brain have recently been identified as a senescence marker for brain tissue in mice [6]. Furthermore, age-related upregulation of miR-34a has also been reported in the liver of aging rats [7] and the heart and spleen of older mice [8]. Liu et al. reported that miR-34a regulates age-associated events and long-term brain integrity in Drosophila, presenting a link between aging and neurodegeneration [9]. The neurosensory retina of the eye is an extension of the brain, and comprises a variety of neurons, which include photoreceptors and ganglion cells [10]. In this study, we examined age-related gene expression of miR-34a in the mouse retina and the RPE, and found a steady increase from 4 months to 24 months of age. A slight decrease in expression was observed between 24 and 32 months of age, although that level was still higher than at 4 months of age. In situ hybridization data supported this age-related upregulation of miR-34a expression consistent with an increase in labeling intensity with age.

Correspondence to: Zeljka Smit-McBride, Vitreoretinal Research Laboratory, UC Davis Department of Ophthalmology, Davis, CA 95616; Phone: (530) 320-8474; FAX: (530) 752-2270; email: zsmcbride@ucdavis.edu

METHODS

Animals and tissue: C57BL/6J mice were obtained from the Jackson Laboratory (Bar Harbour, ME) and from the National Institute of Aging (NIA; Bethesda, MD), while frozen eyes were obtained from BioReliance (Rockville, MD). Mice were housed at 21 °C, under a 12 h:12 h light-dark cycle, with food and water supplied ad libitum. Mice were euthanized by aphyxiation in an air-tight box using CO_2 gas delivered at a flow rate that replaced 20% of the chamber volume/min. For RT-PCR experiments, mouse eyes, ages 4, 18, 24, and 32

months, were processed as previously described [11]. Immediately after euthanization, freshly enucleated eyes were cut along the limbus to separate the ciliary body and the lens from the retina and the RPE/choroid. The retina was then separated from the RPE/choroid, and each tissue was stored separately in RNAlater at −20 °C. Minor modifications for frozen eyes consisted in thawing them overnight in RNAlater ICE (Ambion,Carlsbad, CA) and subsequently moving them to RNAlater (Sigma-Aldrich, St. Louis, MO) followed by dissection, as described above. For in situ hybridization experiments, fresh mouse eyes were collected and processed for paraffin embedding. Each age group had three animals as biologic replicates. Research was conducted in compliance with the ARVO Statement for the Use of Animals in Ophthalmic and Vision Research. This research was authorized by the Institutional Animal Care and Use Committee at the University of California, Davis, CA.

RNA extraction and real-time PCR: Total RNA and microRNA fractions from the retina and the RPE/choroid were extracted and purified using the Qiagen miRNeasy isolation kit (Qiagen, Valencia, CA) following the manufacturer's protocol for separate purification of these two RNA populations. The quantity and quality of RNAs in each fraction were checked using the Agilent 2100 BioAnalyzer RNA kits: the Agilent Small RNA Kit for microRNAs and the Agilent RNA 6000 Nano Kit for total RNA (Agilent, Santa Clara, CA).

In the microRNA RT–PCR analysis, each microRNA sample was amplified using TaqMan preamplification procedure and TaqMan panel A primers (Applied Biosystems, Life Technologies, Grand Island, NY). The TaqMan assays performed were miR-34a (ABI No. 000,426, hsa-miR-34a) and three control genes, *sno-135* (ABI No. 000,460; hsa-miR-135a), *sno-202* (ABI No. 002,579, mmu-miR-202–5), and *U6* (ABI No. 001,973, U6 snRNA). MiRNA assays were conducted at a dilution of 1:1,000. A no enzyme control in the reverse transcriptase (RT) step was included as a negative control.

In the mRNA RT–PCR analysis, reverse transcription was performed using the QuantiTect Reverse Transcription Kit (Qiagen, Valencia, CA). The TaqMan assay performed was Sirt1 (ABI No. Mm00490758_m1) and three reference genes, *Gapdh* (ABI No. Mm99999915_g1), *B2M* (ABI No. Mm00437762_m1), and *Hprt1* (ABI No. Mm00446968_m1). The amplification curves were analyzed using the AB SDS software (Applied Biosystems, Life Technologies) to determine the threshold cycle (C_t)values. All miRNA and mRNA samples had three biologic replicates, and each biologic replicate was also run in triplicate; therefore, the data for each time point are an average of nine individual replicate runs, in accordance with recommendations for RT–PCR best practices [12].

Tissue preparation for in situ hybridization: Three male mice at 4, 18, and 24 months of age were used. Eyes were collected under RNase-free conditions and placed in 10% neutral buffered formalin (Sigma Aldrich) overnight at room temperature in tissue cassettes. After fixation, the eyes were removed from formalin and washed with 0.1 M PBS (HyClone Laboratories, South Logan, UT, catalog # SH30256.01) without Magnesium, Calcium and Phenol Red, (1X: 1.0581 mM Potassium Phosphate Monobasic, 154.0041 mM Sodium Chloride, 5.6002 mM Sodium Phosphate Dibasic, pH range 7.0-7.2) 2X for 15 min each. The eyes were then dehydrated through a series of graded ethanols and cleared in xylene before being embedded in paraffin with known orientation. All mouse eyes were cut in a sagittal plane through or near the optic nerve at 6 µm under RNase-free conditions by thoroughly wiping down the microtome, forceps, water bath, etc., with RNase Zap (Ambion, Life Technologies, Carlsbad, CA) and using RNase-free water (Ambion, Life Technologies) for floating sections. Sections were mounted on SuperFrost Plus (Fisher Scientific, Pittsburgh, PA) slides obtained from a newly opened package.

MicroRNA in situ hybridization: Paraffin sections were air-dried at room temperature for 1.5 h and stored at 4 °C until the day before in situ hybridization, at which point they were hotplated at 60 °C for 45 min, returned to 4 °C, and used the following day. In situ hybridization was implemented according to the guidelines stated in the miRCURY LNA microRNA ISH Optimization Kits (FFPE) protocol (Exiqon, Woburn, MA). Slides were treated with Proteinase K at 15 µg/ml for 10 min at 37 °C. Hybridization was performed at 54 °C for the following: 5′-digoxigenin (DIG) labeled (U6) and double DIG (scrambled and miR-34a), LNA-modified oligonucleotide ISH probes. The following probe concentrations were used: LNA scrambled probe (40 nM), U6 (1 nM), and miR-34a (60 nM). Positive probe labeling was blue/purple. Nuclei were visualized using Nuclear Fast Red counterstain (Vector Laboratories Inc., Burlingame, CA)

Tissue preparation for immunohistochemistry: Three male mice at 4, 18, and 24 months of age were used. Eyes were collected and for orientation in paraffin, the superior region of each eye was marked using tissue dye (The Davidson Marking System, Bradley Products, Bloomington, MN, catalog #1003–6) before enucleation with curved scissors. Each excised eye was fixed in 10% neutral buffered formalin overnight at room temperature before being embedded in paraffin as follows: 2×15 min in PBS, 2×15 min in 50%

ethanol, 2×15 min in 75% ethanol, 2× 15 min in 95% ethanol, 2×15 min in 100% ethanol, 2×15 min in xylene, and 3×40 min in paraffin. Each eye was placed in a paraffin mold in an orientation-specific manner. First, the eye was manipulated so that the previous corneal marking was in the 12 o'clock position. Next, the eye was rotated so that the anterior segment faced the right side of the mold before the embedding ring was placed on top, thus preserving the orientation of the eye, such that when the mold was released from the block, the superior orientation was maintained, and a sagittal section made of the eye when the block was sectioned. Sections were cut using a Leica RM2125RT microtome (Leica, Nussloch, Germany) at 6 µm. Due to the previous orientation of each eye in the paraffin-embedding step, a section through the optic disc represented a sagittal section.

Sirt1 immunohistochemistry: Briefly, sections were placed on SuperFrost Plus microscope slides (Thermo Fisher Scientific, Waltham, MA) and dried overnight at room temperature. Sections were deparaffinized in xylene and hydrated through gradient alcohols, and washed in PBS. Antigen retrieval was performed at 98 °C using 1X Dako Target Retrieval Solution (DakoCytomation, Carpinteria, CA, catalog # S1699) for 20 min and left at room temperature for 20 min before washing with PBS containing 0.05% Tween 20 (Sigma-Aldrich). Finally, the slides were blocked using 5% donkey serum in PBS buffer for 3 h at room temperature.

The slides were incubated in 2 µg/ml rabbit anti-human SIRT1 (LifeSpan BioSciences, Seattle, WA, catalog # LS-B1564) diluted in blocking buffer overnight at 4 °C. After primary antibody exposure, sections were washed in PBS containing 0.1% Tween-20, and then incubated with 6 µg/ml biotinylated donkey anti-rabbit IgG immunoglobulin (Jackson ImmunoResearch, West Grove, PA, catalog # 711–065–152) diluted in PBS containing 0.05% Tween-20 for 30 min, washed, and incubated for 30 min in Vectastain ABC-AP reagent (Vector Laboratories, Burlingame, CA, catalog # AK-5000). Negative controls consisted of an isotype-matched immunoglobulin used at the same concentration as the primary antibody. Color was developed using the BCIP/NBT alkaline phosphatase substrate (Vector Laboratories, catalog # SK-5400). The slides were then washed, counter-stained with Nuclear Fast Red (Vector Laboratories, catalog # H-3403), washed again, dehydrated, cleared in xylene, and coverslipped using VectaMount permanent mounting media (Vector Laboratories, catalog # H-5000).

RESULTS

RT-PCR of miR-34a in the mouse retina: Expression of miR-34a was upregulated with age in the retina at 18, 24, and 32 months when compared to 4 months (Figure 1A). Differences in miR-34a expression levels between the 4- and 24-month-old retinas were statistically significant at $p<0.01$. The largest fold change (FC) was observed in the retina at 24 months compared to 4 months (FC=15.04). The 32-month-old retina still showed upregulation compared to the 4-month-old retina (FC=3.18); however, there was downregulation at 32 months compared to 24 months.

RT-PCR of miR-34a in the mouse RPE/choroid: MiR-34a was upregulated with age in the RPE/choroid at 18 and 24 months compared to 4 months (Figure 1B). Differences in miR-34a expression levels between 4 and 24 months were statistically significant at $p<0.01$. The largest fold change (FC=9.16) was observed between the 24- and 4-month-old age group. However, miR-34a was downregulated at 32 months when compared to 24 months. The expression level of miR-34a in the RPE/choroid at 32 months was similar to that observed at 4 months.

In situ hybridization of miR-34a in the mouse retina: Figure 2 illustrates in situ hybridization (ISH) results of miRNA-34a in the mouse retina at 4, 18, and 24 months. ISH localized miR-34a expression mainly to the cytoplasm of individual cells, and it appeared confined to specific regions within the retina. In the 4-month-old mouse, miR-34a expression had a strong signal in the photoreceptor inner segments (ISs) and scarcely in the outer nuclear layer (ONL; see the inset in Figure 2B) of the retina. In the 18-month-old mouse retina (Figure 2D), distribution was observed in the ganglion cell layer (GCL), inner nuclear layer (INL), and photoreceptor ISs, with the addition of diffused labeling visible in the outer nuclear layer (ONL). Expression levels at 18 months were greatly increased as evidenced by the strong, definitive labeling pattern. In the 24-month-old retina (Figure 2F), distribution was seen in the GCL, INL, ONL, and ISs, and the overall intensity of labeling appeared to be stronger when compared to the 18-month-old mouse retina. MiRNA-34a expression increased with age, especially in the photoreceptor ISs.

In situ hybridization of miR-34a in the mouse RPE: Figure 3 illustrates ISH results for the RPE layer at 4, 18, and 24 months. MiR-34a expression within the RPE layer exhibited age-related upregulation. In the 4-month-old mouse retina (Figure 3B), labeling is barely visible in the cytoplasm surrounding the nucleus of the RPE. By 18 months of age (Figure 3D), the labeling is much more intense and noticeable and is even more pronounced at 24 months (Figure 3F). These

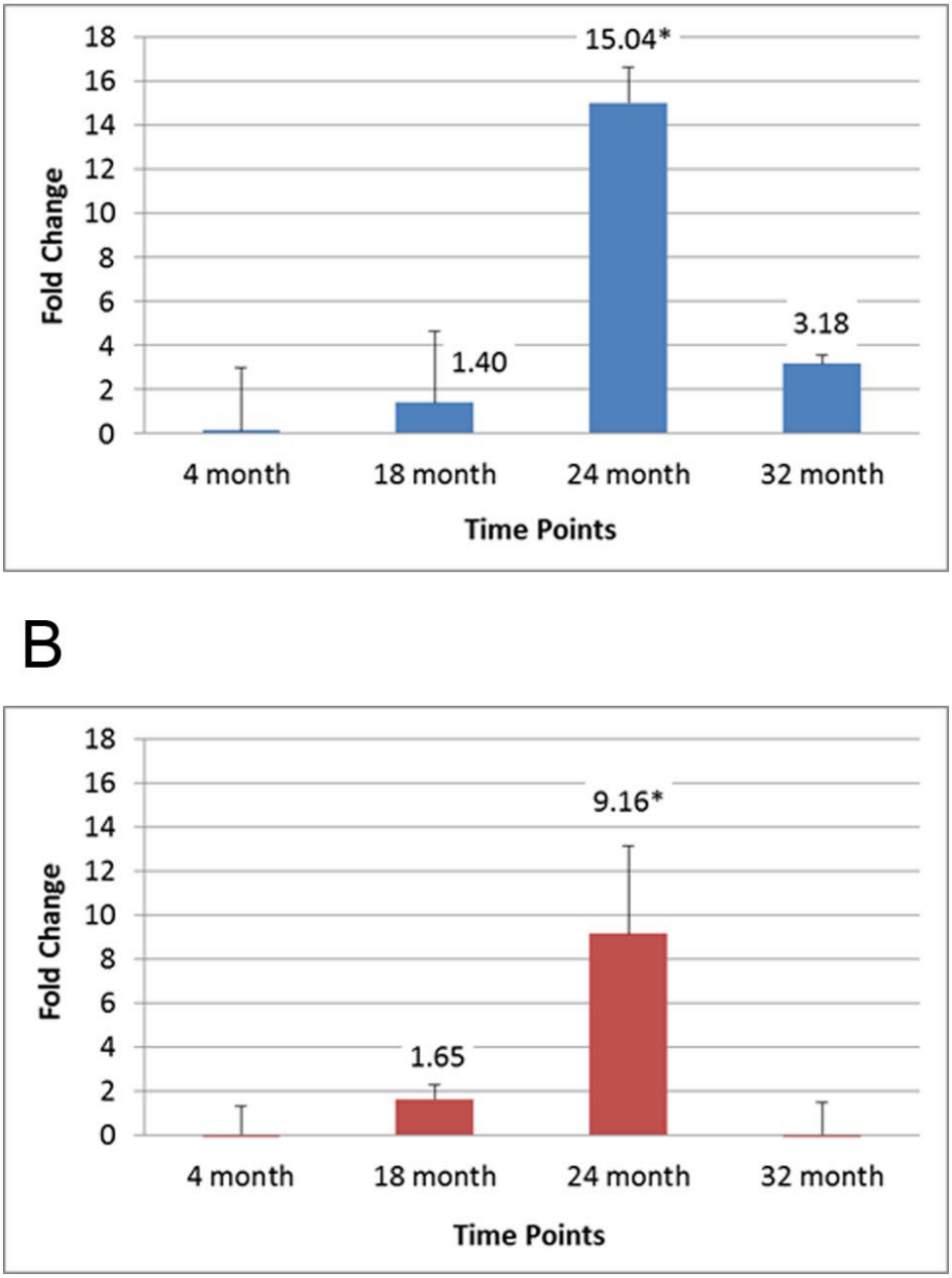

Figure 1. Real-time PCR (RT-PCR) results for the expression of miR-34a in the aging posterior mouse eye. RT–PCR of the retina (**A**) and RPE/choroid (**B**) of isolated miRNA samples at 4, 18, 24, and 32 months of age. There were three samples (n=3) for each of the four time points, for a total of twelve animals (n=12). miRNA samples from each animal tissue at each time point were run in triplicate, resulting in each time point representing an average of nine data values. Data were normalized to a geometric mean of three control small RNAs (U6, sno-202, and sno-135) and calibrated to the 4-month-old sample. The y-axis represents the fold change compared to the 4-month-old sample. * denotes statistically significant differences ($p<0.01$). Error bars represent standard deviation (SD) values.

results are in agreement with the RT–PCR data and indicate upregulation of miR-34a in the RPE with aging.

RT–PCR of miR-34a target mRNA, Sirt1, in the mouse retina and RPE: Age-related change in the expression of the miR-34a target mRNA, Sirt1, was analyzed using RT–PCR (Figure 4). The Sirt1 mRNA showed more than a twofold upregulation in the retina (Figure 4A) and more than a fivefold upregulation in RPE (Figure 4B) at 18 months compared to the 4-month-old animals. Differences in the Sirt1 mRNA expression levels between 4 and 18 months were statistically significant for the retina and the RPE ($p<0.01$; Figure 4A,B, respectively). The level of expression dropped at 24 months in the retina (FC=0.40) and the RPE (FC=–1.84). The downregulation of Sirt1 mRNA expression in the RPE at 24 months was

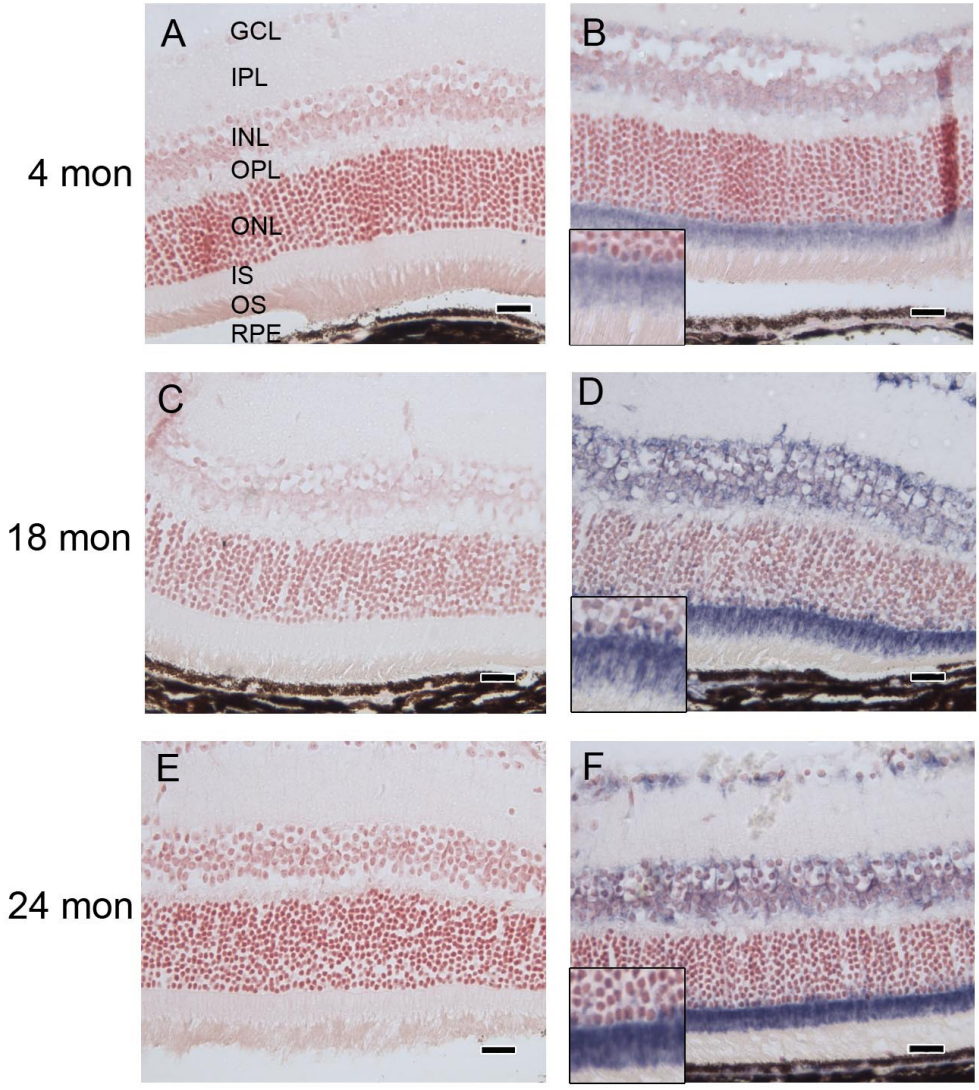

Figure 2. Visualization of miR-34a expression in the mouse retina using in situ hybridization. Paraffin sections of the mouse retina were examined using in situ hybridization at 4, 18, and 24 months of age. Images are from the ventral region near the optic nerve. There were three samples (n=3) for each of the three time points, for a total of nine animals (N=9). The representative images are shown. A scrambled probe was used as a negative control for each time point at 4 (**A**), 18 (**C**), and 24 months (**E**) of age. Negative controls did not label; the pink staining is Nuclear Fast Red stain. A miR-34a probe was used to localize miR-34a expression at 4 (**B**), 18 (**D**), and 24 months (**F**) of age. MiR-34a labeling is blue/purple, and the nuclear counterstain is pink. At 4 months (**B**), miR-34a expression is localized in the inner segments (IS) and scarcely in the outer nuclear layer (ONL; see inset) of the retina. By 18 months (**D**), expression is observed in the ganglion cell layer (GCL), inner nuclear layer (INL), and more intensely in the IS and the ONL. At 24 months (**F**), miR-34a expression is in the GCL and the INL, with more intensity and strong expression in the IS and the ONL. Scale bar=20 µm.

statistically significant compared to 4 months (FC=–1.84; $p<0.05$). The level of expression of Sirt1 mRNA at 32 months in the retina and the RPE returned to the same level as that of the 4-month-old animals.

Immunohistochemistry of Sirt1 protein, sirtuin 1 in the retina and RPE: Age-related changes in the level of expression and tissue distribution were examined for one of the miR-34a regulatory targets, Sirt1 protein or sirtuin 1, using immunohistochemistry approach on the paraffin sections of mouse eyes (Figure 5). The level of sirtuin 1 expression was increased at 18 and 24 months compared to 4 months. The Sirt1 protein was detected in the outer limiting membrane (OLM), outer plexiform layer (OPL), occasional nuclei in the INL, and inner plexiform layer (IPL; Figure 5B,D,F). There was an increase in the level of Sirt1protein labeling along the basal side of the RPE (inserts in Figure 5B,D,F) with age.

Statistical analysis: For the RT–PCR experiments, RNA was isolated from each tissue from three animals (biologic replicates) at four ages for a total of 12 animals. Each sample for RT–PCR analysis was performed using three biologic replicates, and each biologic replicate was run in triplicate. Therefore, the data for each time point were an average of nine individual replicate runs. Raw RT–PCR data for miR-34a expression were normalized to the geometric mean of the three control small RNAs (sno-135, sno-202, and U6) and calibrated to 4-month-old samples. To test our hypothesis

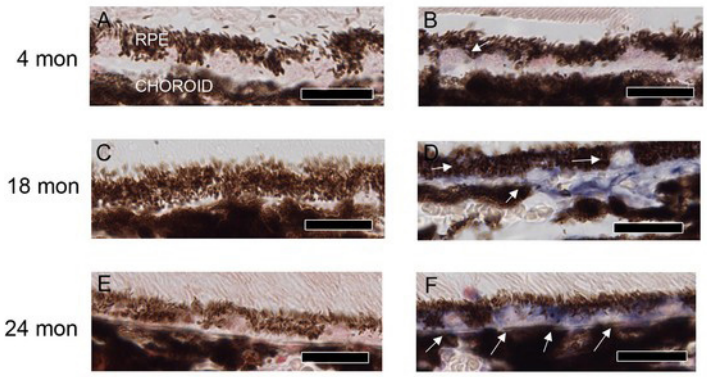

Figure 3. Visualization of miR-34a expression in the mouse RPE using in situ hybridization. Paraffin sections of the mouse RPE were examined using in situ hybridization at 4, 18, and 24 months of age. Images are from the ventral region near the optic nerve. There were three samples (n=3) for each of the three time points, for a total of nine animals (N=9). The representative images are shown. A scrambled probe was used as a negative control for each time point at 4 (**A**), 18 (**C**), and 24 months (**E**) of age. Negative controls did not label; pink staining is Nuclear Fast Red. A miR-34a probe was used to localize miR-34a expression at 4 (**B**), 18 (**D**), and 24 months (**F**) of age. MiR-34a labeling is blue/purple (indicated with white arrows), and the nuclear counterstain is pink. At 4 months (**B**), barely perceptible miR-34a expression is seen in the cytoplasm of the RPE cells. By 18 months (**D**), expression is much more visible and still in the cytoplasm. At 24 months (**F**), miR-34a expression is visibly pronounced and remains cytoplasmic. Scale bar=20 µm.

that miR-34a expression increases with age, a pairwise *t* test for statistical significance between the aged groups was performed using a one-tailed unpaired Student *t* test. Statistically significant differences were defined as $p<0.05$. To ensure that our number of biologic replicates could detect significant changes in the levels of miR-34A expression, these data were used to perform power calculations. Power and sample size calculations were performed using the online statistical tool, Power & Sample Size Calculator, from Statistical Solutions. When the mean value of 14 for the 24-month-old animals and the mean value of 0.5 for 4-month-old animals were considered, using the power of 0.8, the sample size for the test was calculated at n=1. When n=3 was entered, our sample size for each age group, the power of the test was calculated at 1. These calculations show that three biologic replicates at each age, given the standard means that were experimentally determined, satisfied the requirements for power in our experimental design. The same protocol was followed for Sirt1 RT–PCR, except that the three reference genes were *Gapdh*, *B2M*, and *Hprt1*.

DISCUSSION

We have provided a report on the age-related changes of miR-34a expression in the normal adult C57BL/6J mouse retina and RPE. MiR-34a expression increased with age in the retina and the RPE up to 24 months of age, and the results were consistent for RT–PCR and ISH. Our results agree with the work of Li et al. [6], who identified miR-34a as a noninvasive biomarker for brain aging in C57BL/6J mice. They showed that the miR-34a temporal increase in expression could be detected in peripheral blood mononuclear cells (PBMCs) and plasma samples, which correlates with the increase in neural tissue of the brain. Our results confirmed this for neural tissue in the eye, specifically the neuroretina and the RPE.

It is interesting that another process described in the mouse retina, as well as the RPE/choroid, follows a similar time course as miR-34a, increased mitochondrial DNA (mtDNA) oxidative damage and an age-related decrease/deficiency of DNA repair enzymes [14,15], as a function of normal aging. Wang et al. demonstrated increased damage to mtDNA in the GCL, INL, and ISs of mouse photoreceptors with age, as well as the RPE. These are the same regions where we observed the strongest upregulation of the intensity of labeling of miR-34a with age. Wang et al. observed colocalization of 8-OHdG, an indicator of oxidative DNA damage, and manganese superoxide dismutase (MnSod) in the photoreceptor ISs that was intense in old retinas compared to young retinas, which corresponded with our findings of miR-34a upregulation in older retinas. This makes sense since the photoreceptor ISs contain a high density of mitochondria [16]. This suggests that miR-34a may play a role in senescence and in increased oxidative damage to the aging retina and the RPE.

MiR-34a expression decreased between 24 and 32 months of age in the retina and the RPE (Figure 1A,B, respectively). Although the expression was still higher than at 4 months, the level of expression at 32 months decreased to the same level as observed in the 18-month-old retina and below that for the 18-month-old RPE/choroid. This downregulation of the level of expression of miR-34a could be the result of age-related

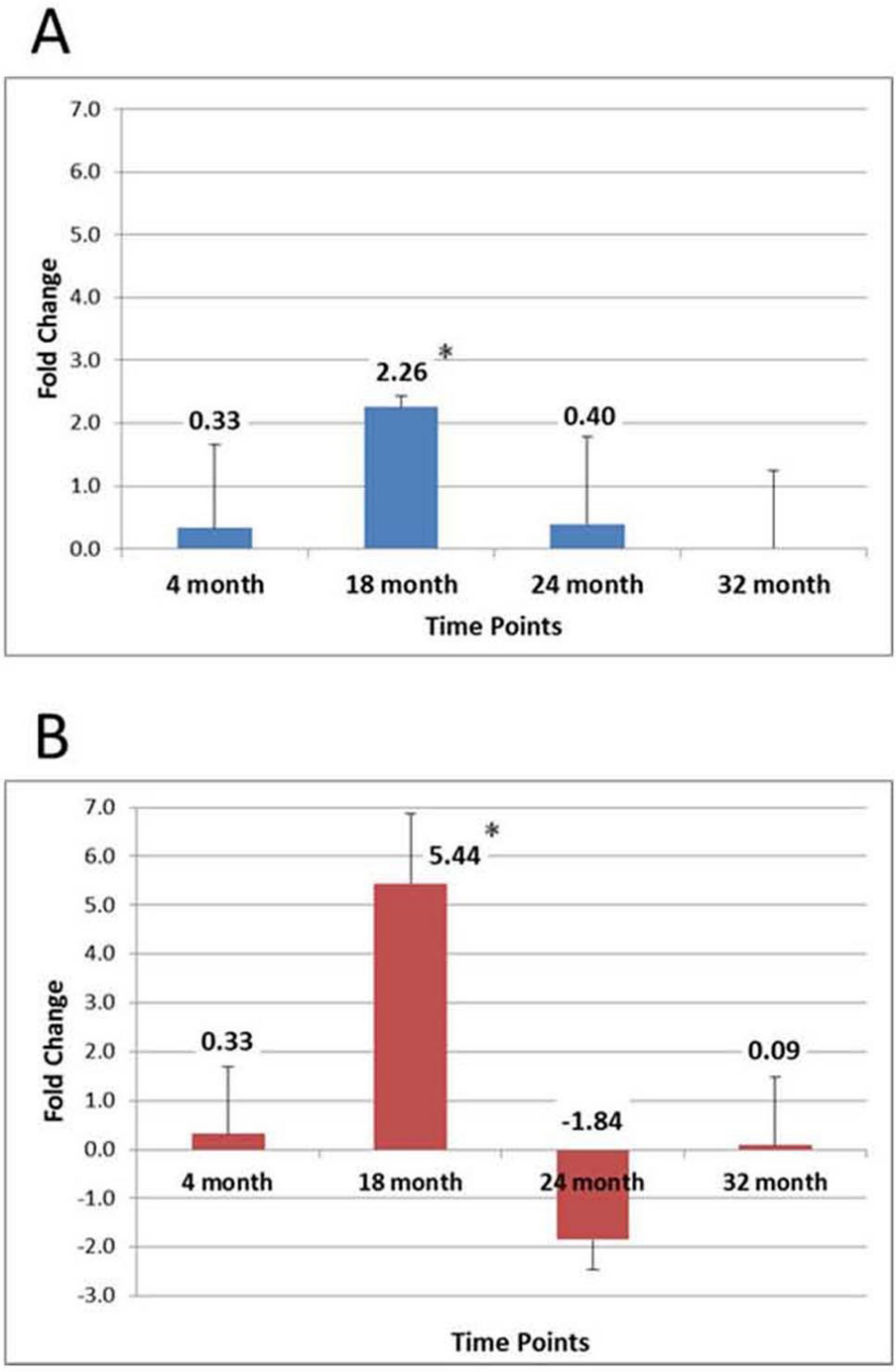

Figure 4. Real-time PCR (RT-PCR) results for the expression of miR-34a target mRNA Sirt1 in the aging posterior mouse eye. RT–PCR of the retina (**A**) and RPE/choroid (**B**) isolated total RNA samples at 4, 18, 24, and 32 months of age. There were three samples (n=3) for each of the four time points, for a total of twelve animals (n=12). Total RNA samples from each animal tissue at each time point were run in triplicate, resulting in each time point representing an average of nine data values. Data were normalized to a geometric mean of the three control genes (*Gapdh*, *B2M*, and *Hprt1*) and calibrated to the 4-month-old sample. The y-axis represents the fold change compared to the 4 month old. * denotes statistically significant differences ($p<0.01$). Error bars represent standard deviation (SD) values.

epigenetic regulatory changes or epigenetic drift in the regulatory regions of the miR-34a gene, i.e., methylation of the CpG islands that the miR-34a promoter is embedded in, as happens in squamous cell carcinoma [17] and many other cancers [18].

The observation that miR-34a is downregulated in the mouse eye with advanced age is novel, but the significance of this observation is not clear. There are opposing streams of evidence as to whether a high level of expression of miR-34a is beneficial or deleterious to the cells. High levels

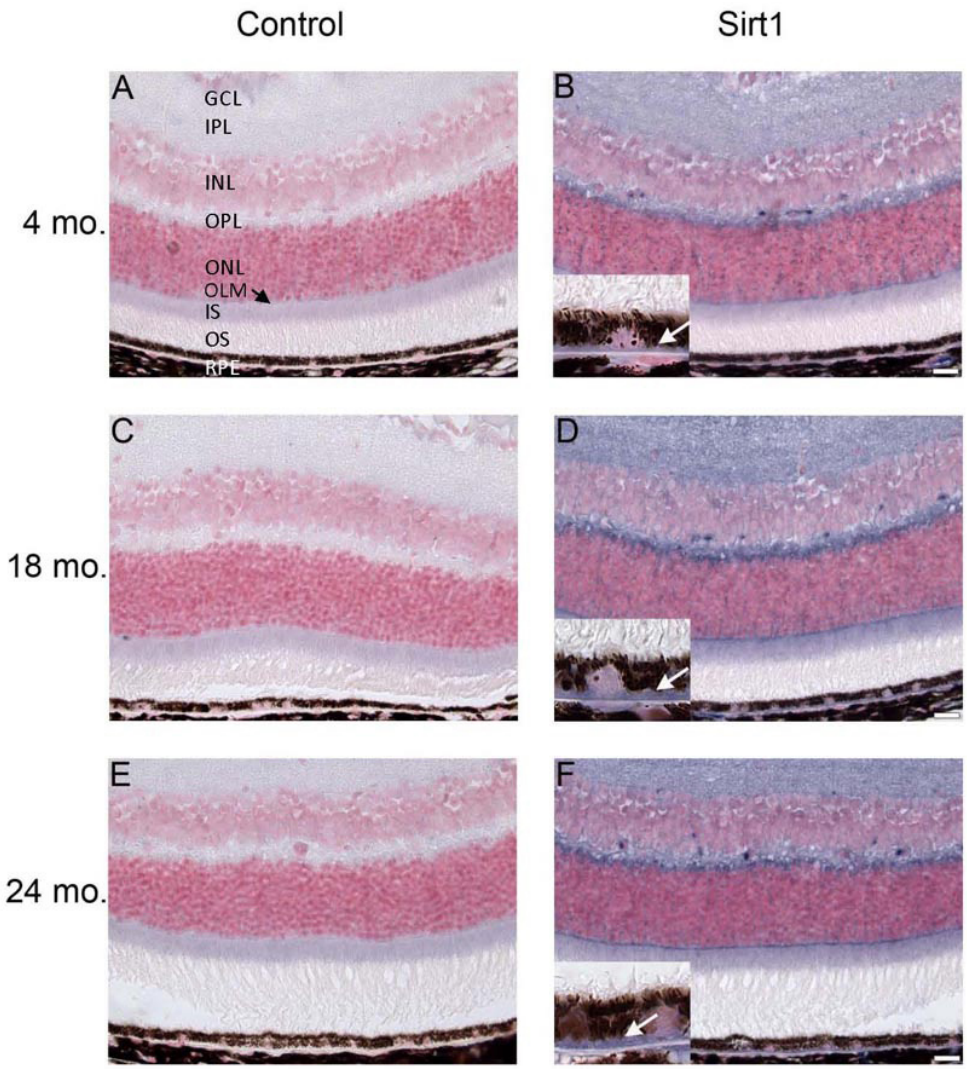

Figure 5. Sirt1 immunohistochemistry in the aging posterior mouse eye. There were three samples (n=3) for each of the three time point, for a total of nine animals (N=9). The representative images are shown. Sagittal sections near the optic nerve of 4- (**B**), 18- (**D**), and 24- (**F**) month-old mice were immunolabeled using a rabbit anti-human SIRT1 antibody that cross reacts with mouse tissue. Sirt1 labeling was observed along the basal edge of the RPE (white arrows). Sirt1 was also detected in the OLM (black arrow), the OPL, occasional nuclei in the INL, and the IPL. Negative controls using isotype-matched rabbit immunoglobulin (IgG) at the same concentration as the SIRT1 antibody are shown for the 4- (**A**), 18- (**C**), and 24- (**E**) month-old animals. Scale bar=20 µm. OLM=outer limiting membrane, OPL=outer plexiform layer, INL=inner nuclear layer, IPL=inner plexiform layer.

of miR-34a expression inhibit the cell cycle, which might be beneficial to an organism with cancer or age-damaged cells. MiR-34a has been described as a tumor suppressor because its upregulation induces apoptosis in several types of cancer cells [19,20]. Yamakuchi et al. have shown that miR-34a regulates silent information regulator 1 (Sirtuin or SIRT1) expression [21]. MiR-34a inhibits SIRT1 expression through a miR-34a-binding site within the SIRT1 3′ UTR, leading to an increase in acetylated p53 and expression of transcriptional targets of p53 that regulate the cell cycle and apoptosis. Interestingly, miR-34a itself is a transcriptional target of p53, suggesting a positive feedback loop between p53 and miR-34a [22]. Thus, miR-34a functions as a tumor suppressor, in part, through a SIRT1-p53 pathway.

However, another body of research suggests that high levels of miR-34a expression might be deleterious to cells. Although miR-34a increases with age, its prime target, Sirt1, decreases, creating an inversely proportional relationship [6]. Our data support that statement. We found an inversely proportional relationship between the levels of expression of miR-34a and Sirt1 mRNA in the retina and the RPE at 18 months and 24 months of age. Although miR-34a showed mild upregulation at 18 months in the retina and the RPE and maximum expression in the 24-month-old retina and RPE compared to the 4-month-old retina and RPE (Figure 1A,B), Sirt1 showed exactly the opposite (Figure 4A,B). Sirt1 expression was highest at 18 months in the retina and RPE, while expression decreased at 24 months to the same level in the retina or less in the RPE, as the 4-month-old animals.

Sirt1 has been identified as playing an important role in protecting cells from oxidative stress and DNA damage [21], which accumulates with time. Several animal studies have

examined the role of Sirt1 in the aging eye, and an excellent review of the current knowledge about Sirt1 and ocular aging was provided by Mimura et al. [23]. Sirt1 is expressed in retinal cells, as well as other ocular tissues, and upregulation of Sirt1 in animal models provides a protective effect against various ocular diseases, such as retinal degeneration, optic neuritis, and uveitis [23]. According to these authors, downregulation of miR-34a would be beneficial and neuroprotective for the eye, since it would increase the availability of the protective Sirt1 protein. Hou et al. showed that high levels of miR-34a can lead to inhibition of the proliferation and migration of ARPE-19 cells through downregulation of some of the target cell cycle genes [24], which might be an obstacle to RPE cell growth and the repair process in the aging eye.

Our examination of the sirtuin 1 age-related change of expression and distribution in the eye using immunohistochemistry showed an increase in expression at 18 and 24 months compared to 4-month-old animals (Figure 5). We observed an age-related increase in labeling in the OPL and the OLM. In the RPE, we observed cytoplasmic age-related accumulation of Sirt1 labeling in the basal region of the RPE, above Bruch's membrane. Localization of Sirt1 in retinal tissue is somewhat controversial. Cytoplasmic localization of Sirt1 in the adult retina has been observed by Maloney et al. [25], while Jaliffa et al. described Sirt1 localization as mainly nuclear in the normal mouse retina [26]. We realized that immunohistochemistry does not represent a quantitative measurement, and as a result, we do not have a basis for statistically treating these data for significance.

In conclusion, our results show that miR-34a is a putative aging biomarker for the retina and the RPE in the mouse. Furthermore, these results taken together suggest that miR-34a represents an attractive potential aging marker, modulation of which might become an interesting target for further research in protection against ocular diseases related to oxidative stress-induced retinal damage.

ACKNOWLEDGMENTS

This work was supported by grants from NIH R01EY021024 and R01EY021537 to LMH and ZSM, UC Davis AF IDEA Grant to ZSM, an Unrestricted Grant from Research to Prevent Blindness, to the Dept. of Ophthalmology, UC Davis School of Medicine, and NEI Core Facilities grant P30-EY012576 (UCD). Work at UC Davis was conducted in a facility constructed with support from Research Facilities Improvement Program Grant Number C06 RR-12088–01 from the National Center for Research Resources, National Institutes of Health. This data was presented in a preliminary form at ARVO 2013 and 2014 and ISER 2014 as poster presentations.

REFERENCES

1. Chen LH, Chiou GY, Chen YW, Li HY, Chiou SH. MicroRNA and aging: a novel modulator in regulating the aging network. Ageing Res Rev 2010; 9:Suppl 1S59-66. [PMID: 20708718].
2. Smith-Vikos T, Slack FJ. MicroRNAs and their roles in aging. J Cell Sci 2012; 125:7-17. [PMID: 22294612].
3. Menghini R, Casagrande V, Cardellini M, Martelli E, Terrinoni A, Amati F, Vasa-Nicotera M, Ippoliti A, Novelli G, Melino G, Lauro R, Federici M. MicroRNA 217 modulates endothelial cell senescence via silent information regulator 1. Circulation 2009; 120:1524-32. [PMID: 19786632].
4. Olivieri F, Spazzafumo L, Santini G, Lazzarini R, Albertini MC, Rippo MR, Galeazzi R, Abbatecola AM, Marcheselli F, Monti D, Ostan R, Cevenini E, Antonicelli R, Franceschi C, Procopio AD. Age-related differences in the expression of circulating microRNAs: miR-21 as a new circulating marker of inflammaging. Mech Ageing Dev 2012; 133:675-85. [PMID: 23041385].
5. Toledano H. The role of the heterochronic microRNA let-7 in the progression of aging. Exp Gerontol 2013; 48:667-70. [PMID: 22960398].
6. Li X, Khanna A, Li N, Wang E. Circulatory miR34a as an RNAbased, noninvasive biomarker for brain aging. Aging (Albany, NY) 2011; 3:985-1002. [PMID: 22064828].
7. Li N, Muthusamy S, Liang R, Sarojini H, Wang E. Increased expression of miR-34a and miR-93 in rat liver during aging, and their impact on the expression of Mgst1 and Sirt1. Mech Ageing Dev 2011; 132:75-85. [PMID: 21216258].
8. Ito T, Yagi S, Yamakuchi M. MicroRNA-34a regulation of endothelial senescence. Biochem Biophys Res Commun 2010; 398:735-40. [PMID: 20627091].
9. Liu N, Landreh M, Cao K, Abe M, Hendriks GJ, Kennerdell JR, Zhu Y, Wang LS, Bonini NM. The microRNA miR-34 modulates ageing and neurodegeneration in Drosophila. Nature 2012; 482:519-23. [PMID: 22343898].
10. Hildebrand GD, Fielder AR. Anatomy and Physiology of the Retina. In: Reynolds J, Olitsky S, editors. Pediatric Retina. Heidelberg: Springer-Verlag Berlin; 2011. p. 39–65.
11. Smit-McBride Z, Oltjen SL, Lavail MM, Hjelmeland LM. A strong genetic determinant of hyperoxia-related retinal degeneration on mouse chromosome 6. Invest Ophthalmol Vis Sci 2007; 48:405-11. [PMID: 17197561].
12. Bustin SA, Benes V, Garson JA, Hellemans J, Huggett J, Kubista M, Mueller R, Nolan T, Pfaffl MW, Shipley GL, Vandesompele J, Wittwer CT. The MIQE guidelines: minimum information for publication of quantitative real-time PCR experiments. Clin Chem 2009; 55:611-22. [PMID: 19246619].
13. Chen H, Liu B, Lukas TJ, Neufeld AH. The aged retinal pigment epithelium/choroid: a potential substratum for the

pathogenesis of age-related macular degeneration. PLoS ONE 2008; 3:e2339-[PMID: 18523633].

14. Wang AL, Lukas TJ, Yuan M, Neufeld AH. Age-related increase in mitochondrial DNA damage and loss of DNA repair capacity in the neural retina. Neurobiol Aging 2010; 31:2002-10. [PMID: 19084291].

15. Hoang QV, Linsenmeier RA, Chung CK, Curcio CA. Photoreceptor inner segments in monkey and human retina: mitochondrial density, optics, and regional variation. Vis Neurosci 2002; 19:395-407. [PMID: 12511073].

16. Chen X, Hu H, Guan X, Xiong G, Wang Y, Wang K, Li J, Xu X, Yang K, Bai Y. CpG island methylation status of miRNAs in esophageal squamous cell carcinoma. Int J Cancer 2012; 130:1607-13. [PMID: 21547903].

17. Suzuki H, Maruyama R, Yamamoto E, Kai M. DNA methylation and microRNA dysregulation in cancer. Mol Oncol 2012; 6:567-78. [PMID: 22902148].

18. Welch C, Chen Y, Stallings RL. MicroRNA-34a functions as a potential tumor suppressor by inducing apoptosis in neuroblastoma cells. Oncogene 2007; 26:5017-22. [PMID: 17297439].

19. Chang TC, Wentzel EA, Kent OA, Ramachandran K, Mullendore M, Lee KH, Feldmann G, Yamakuchi M, Ferlito M, Lowenstein CJ, Arking DE, Beer MA, Maitra A, Mendell JT. Transactivation of miR-34a by p53 broadly influences gene expression and promotes apoptosis. Mol Cell 2007; 26:745-52. [PMID: 17540599].

20. Yamakuchi M, Ferlito M, Lowenstein CJ. miR-34a repression of SIRT1 regulates apoptosis. Proc Natl Acad Sci USA 2008; 105:13421-6. [PMID: 18755897].

21. Jain AK, Allton K, Iacovino M, Mahen E, Milczarek RJ, Zwaka TP, Kyba M, Barton MC. p53 regulates cell cycle and microRNAs to promote differentiation of human embryonic stem cells. PLoS Biol 2012; 10:e1001268-[PMID: 22389628].

22. Mimura T, Kaji Y, Noma H, Funatsu H, Okamoto S. The role of SIRT1 in ocular aging. Exp Eye Res 2013; 116:17-26. [PMID: 23892278].

23. Hou Q, Tang J, Wang Z, Wang C, Chen X, Hou L, Dong XD, Tu L. Inhibitory Effect of MicroRNA-34a on Retinal Pigment Epithelial Cell Proliferation and Migration. Invest Ophthalmol Vis Sci 2013; 54:6481-8. [PMID: 23970470].

24. Maloney SC, Antecka E, Odashiro AN, Fernandes BF, Doyle M, Lim LA, Katib Y, Burnier MN Jr. Expression of SIRT1 and DBC1 in Developing and Adult Retinas. Stem Cells Int 2012; 2012:908183-[PMID: 22969813].

25. Jaliffa C, Ameqrane I, Dansault A, Leemput J, Vieira V, Lacassagne E, Provost A, Bigot K, Masson C, Menasche M, Abitbol M. Sirt1 involvement in rd10 mouse retinal degeneration. Invest Ophthalmol Vis Sci 2009; 50:3562-72. [PMID: 19407027].

Articles are provided courtesy of Emory University and the Zhongshan Ophthalmic Center, Sun Yat-sen University, P.R. China. The print version of this article was created on 5 November 2014. This reflects all typographical corrections and errata to the article through that date. Details of any changes may be found in the online version of the article.